EXTENDED PDF FORMAT
SPONSORED BY

BIO-RAD

http://discover.bio-rad.com



The Cause of Carbon Isotope Minimum Events on Glacial Terminations

Howard J. Spero, *et al.*

Science **296**, 522 (2002);
DOI: 10.1126/science.1069401

The following resources related to this article are available online at www.sciencemag.org (this information is current as of November 27, 2006):

Updated information and services, including high-resolution figures, can be found in the online version of this article at:
http://www.sciencemag.org/cgi/content/full/296/5567/522

This article **cites 8 articles**, 1 of which can be accessed for free:
http://www.sciencemag.org/cgi/content/full/296/5567/522#otherarticles

This article has been **cited by** 27 article(s) on the ISI Web of Science.

This article has been **cited by** 2 articles hosted by HighWire Press; see:
http://www.sciencemag.org/cgi/content/full/296/5567/522#otherarticles

This article appears in the following **subject collections**:
Atmospheric Science
http://www.sciencemag.org/cgi/collection/atmos

Information about obtaining **reprints** of this article or about obtaining **permission to reproduce this article** in whole or in part can be found at:
http://www.sciencemag.org/help/about/permissions.dtl

Downloaded from www.sciencemag.org on November 27, 2006

Science (print ISSN 0036-8075; online ISSN 1095-9203) is published weekly, except the last week in December, by the American Association for the Advancement of Science, 1200 New York Avenue NW, Washington, DC 20005. Copyright c 2005 by the American Association for the Advancement of Science; all rights reserved. The title SCIENCE is a registered trademark of AAAS.

References and Notes

1. E. Coronado, J. R. Galan-Mascaros, C. J. Gomez-Garcia, V. Laukhin, *Nature* **408**, 447 (2000).
2. F. Croce, G. B. Appetecchi, L. Persi, B. Scrosati, *Nature* **394**, 456 (1998).
3. T. J. Pinnavaia, *Science* **220**, 365 (1983).
4. Y. Wang, N. Herron, *Science* **273**, 632 (1996).
5. J. G. Winiarz, L. M. Zhang, M. Lal, C. S. Friend, P. N. Prasad, *J. Am. Chem. Soc.* **121**, 5287 (1999).
6. G. Schmid, Ed., *Clusters and Colloids* (Wiley, Weinheim, Germany, 1994).
7. S. N. Sidorov *et al.*, *J. Am. Chem. Soc.* **123**, 10502 (2001).
8. M. B. Shiflett, H. C. Foley, *Science* **285**, 1902 (1999).
9. L. M. Robeson, *J. Membr. Sci.* **62**, 165 (1991).
10. B. D. Freeman, *Macromolecules* **32**, 375 (1999).
11. S. Kulprathipanja, R. W. Neuzil, N. Li, U.S. Patent 4,740,219 (1988).
12. M. Jia, K. V. Peinemann, R. D. Behling, *J. Membr. Sci.* **57**, 289 (1991).
13. R. Mahajan, C. M. Zimmerman, W. J. Koros, in *Polymer Membranes for Gas and Vapor Separation: Chemistry and Materials Science*, B. D. Freeman, I. Pinnau, Eds. (American Chemical Society, Washington, DC, 1999), pp. 277–286.
14. T. Graham, *Philos. Mag.* **32**, 401 (1866).
15. B. D. Freeman, I. Pinnau, *Trends Polym. Sci.* **5**, 167 (1997).
16. A. Morisato, I. Pinnau, *J. Membr. Sci.* **121**, 243 (1996).
17. I. Pinnau, Z. He, U.S. Patent 6,316,684 (2001).
18. V. P. Shantarovich, I. B. Kevdina, Y. P. Yampolskii, A. Y. Alentiev, *Macromolecules* **33**, 7453 (2000).
19. M. H. Cohen, D. Turnbull, *J. Chem. Phys.* **3**1, 1164 (1959).
20. R. M. Barrer, in *Diffusion in Polymers*, J. Crank, G. S. Park, Eds. (Academic Press, New York, 1968), pp. 165–217.
21. C. Maxwell, *Treatise on Electricity and Magnetism* (Oxford Univ. Press, London, 1873), vol. 1.
22. R. M. Barrer, J. A. Barrie, M. G. Rogers, *J. Polym. Sci. Part A* **1**, 2565 (1963).
23. The results presented in Figs. 1 and 2 were highly reproducible. Using a wide variety of gases, we measured the properties of many films as functions of pressure and the number of pressurization and depressurization cycles. Permeability and selectivity did not depend on the number of pressurization and depressurization cycles. Sample-to-sample variability was always within the typical range of experimental uncertainty (±7% for permeability, ±5% solubility, and ±15% for diffusivity).
24. The results in Fig. 2 for films were validated in state-of-the-art thin film composite membranes prepared from mixtures of PMP and fumed silica, and these thin film composite membranes were used to successfully prepare 1-square-meter pilot-scale spiral wound modules.
25. Y. Kobayashi, K. Haraya, S. Hattori, T. Sasuga, *Polymer* **35**, 925 (1994).
26. I. Pinnau, L. G. Toy, *J. Membr. Sci.* **116**, 199 (1996).

27. Funded by NSF (grants DMI-9901788 and CTS-9803225) and the U.S. Department of Energy (grant DE-FG02-99ER14991).

7 January 2002; accepted 12 March 2002

The Cause of Carbon Isotope Minimum Events on Glacial Terminations

Howard J. Spero[1]* and David W. Lea[2]

The occurrence of carbon isotope minima at the beginning of glacial terminations is a common feature of planktic foraminifera carbon isotopic records from the Indo-Pacific, sub-Antarctic, and South Atlantic. We use the $\delta^{13}C$ record of a thermocline-dwelling foraminifera, *Neogloboquadrina dutertrei*, and surface temperature estimates from the eastern equatorial Pacific to demonstrate that the onset of $\delta^{13}C$ minimum events and the initiation of Southern Ocean warming occurred simultaneously. Timing agreement between the marine record and the $\delta^{13}C$ minimum in an Antarctic atmospheric record suggests that the deglacial events were a response to the breakdown of surface water stratification, renewed Circumpolar Deep Water upwelling, and advection of low $\delta^{13}C$ waters to the convergence zone at the sub-Antarctic front. On the basis of age agreement between the absolute $\delta^{13}C$ minimum in surface records and the shift from low to high $\delta^{13}C$ in the deep South Atlantic, we suggest that the $\delta^{13}C$ rise that marks the end of the carbon isotope minima was due to the resumption of North Atlantic Deep Water influence in the Southern Ocean.

A persistent feature of planktic and intermediate-depth benthic foraminifera carbon isotope records from tropical through Southern high latitudes is the large (0.3 to 1.2‰), rapid negative $\delta^{13}C$ excursions that are observed on deglaciations (*1*–*5*). Because these carbon isotope events occur when the northern hemisphere ice sheets are collapsing, it is difficult to explain them via the transfer of isotopically light carbon from the terrestrial to oceanic carbon reservoirs. Rather, since the terrestrial biosphere was already expanding and sequestering ^{12}C-rich CO_2 into biomass, and the glacial oceans were preconditioned with a low $\delta^{13}C$ signature from remineralized terrestrial carbon during ice sheet growth (*6*), one would expect the $\delta^{13}C$ of the oceanic carbon reservoir to increase at the end of glacials. The extensive distribution of these $\delta^{13}C$ minima in the tropical Indo-Pacific, south Atlantic and sub-Antarctic and the rate at which the full signal appears in different basins, suggests the signal source originates from an oceanic region with direct connection to the different ocean basins (*5*).

Ninnemann and Charles (*5*) argued that these carbon isotope minima could not be a whole ocean signal because they are absent from north Atlantic planktonic records. Rather, they suggested that the tropical Indo-Pacific surface $\delta^{13}C$ minima were due to the transfer of a preformed $\delta^{13}C$ signal from the sub-Antarctic via Antarctic Intermediate Water (AAIW) or sub-Antarctic Mode Water (SAMW) (*2, 7*), with subsequent propagation through the low-latitude thermocline. They further proposed that the signal source was a change in gas exchange fractionation across the air-sea interface as Southern Ocean temperatures warmed at the end of glacials. Because a decrease in $^{13}C/^{12}C$ fractionation would accompany a general postglacial oceanic surface temperature (SST) increase, (*5*) predicted that the $\delta^{13}C$ of atmospheric CO_2 should rise as oceanic $\delta^{13}C$ decreased. However, $\delta^{13}C$ data from Late Quaternary packrat middens (*8*) and CO_2 from the Taylor Dome ice core (*9*) show that atmospheric $\delta^{13}C$ initially decreased as the deglaciation began, and did not begin to increase until ~3 thousand years (ky) later. These atmospheric proxies are not consistent with the proposed equilibration mechanism, requiring us to explore alternatives to explain the termination $\delta^{13}C$ events.

Site TR163-19 is located on the Cocos Ridge in the eastern equatorial Pacific (EEP) (2°15.5′N, 90°57.1′W, 2348 m water depth), just north of the cold upwelling water that characterizes much of this region (*10*). Here, the subsurface thermocline waters are thought to be strongly influenced by sub-Antarctic water masses via the equatorial undercurrent (EUC) (*11, 12*) and the region is not complicated by changes in the position of deep ocean currents with different isotopic composition as is the case in the Atlantic Ocean (*13*). The source of the EUC and waters upwelling from the Peru-Chile undercurrent is likely SAMW, which forms north of the sub-Antarctic front and is the major precursor to AAIW (*14*). It is thought that SAMW ventilates the Pacific Ocean as AAIW by subduction and northward advection into the Pacific subtropical gyre from its primary source in the southeast Pacific (*15*). The dense component of SAMW subsequently flows through the Drake Passage where it is slightly modified, finally becoming the main core of AAIW in the Atlantic and Indian Oceans. In the southwest Pacific, older AAIW flows into the Pacific subtropical gyre where it also contributes to the EUC. The nutrient and $\delta^{13}C$ content of Pacific AAIW is set by the chemistry of upwelled circumpolar deep water (CPDW) and partial equil-

[1]Department of Geology, University of California, Davis, CA 95616, USA. [2]Department of Geological Sciences and the Marine Science Institute, University of California, Santa Barbara, CA 93106, USA.

*To whom correspondence should be addressed. E-mail: spero@geology.ucdavis.edu

Downloaded from www.sciencemag.org on November 27, 2006

ibration with atmospheric CO_2 (*16*) as waters advect into the SAMW source region. On the basis of CFC-11 content, part of the AAIW source to the Pacific EUC has a component that is <25 years old (*17*), suggesting that changes in water column chemistry at the sub-Antarctic front will be recorded in the chemistry of EEP foraminifera within a century or less.

In the vicinity of Site TR163-19, EUC waters are found below ~75 m depth (*12*) where a strong halocline, thermocline, and carbonate chemistry chemocline define the boundary between the mixed layer and underlying EUC (Fig. 1) (*18, 19*). The nonspinose species, *Neogloboquadrina dutertrei*, is a common inhabitant of the EEP thermocline with a preferred depth habitat of 60 to 150 m (*19*). As such, *N. dutertrei* records a subsurface thermocline signal derived from the EUC that is distinct from the mixed layer record of *Globigerinoides ruber* at Site TR163-19 (Fig. 2, A and B).

Lea *et al.* (*10*) argued that within the 2 ky resolution of the *G. ruber* samples analyzed at TR163-19, Mg/Ca derived SST and the Vostok ice core deuterium record (*20*), a proxy for Antarctic temperature, are coherent with no discernible phase lag for the past 260 ky. This implies that in the eastern tropical Pacific, SST changes synchronously with temperatures over Antarctica and the Southern Ocean. Model results (*21*) and observations from Greenland ice cores (*22*) show that high-latitude warming and sea ice melt back can occur on time scales of decades. If these interpretations and models are correct, then geochemical signals transmitted from the Southern Ocean into the EEP via the EUC-SAMW/AAIW connection should be synchronous with Southern Ocean circulation changes south of the sub-Antarctic front.

Comparison of the *N. dutertrei* $\delta^{13}C$ record with the Mg/Ca SST reconstruction from *G. ruber* (*10*) (Fig. 2B) shows that on both glacial Termination I and II, the intervals immediately prior to the initiation of the $\delta^{13}C$ minimum events coincide with the final interval of cool glacial SST. Because the SST rise and $\delta^{13}C$ decrease occur in the same intervals of one core, there is no ambiguity about the relative timing of the events. Radiocarbon dating of the sediment interval just prior to the $\delta^{13}C$ decrease and SST rise yields a ^{14}C age of 16,630 ± 50 years before the present (70 cm), equivalent to 19.8 ± 0.3 calendar ky (*23*). The $\delta^{13}C$ minimum itself occurs at a ^{14}C age of 13,250 ± 40 (53 cm), equivalent to 15.9 ± 0.2 calendar ky (Fig. 3A). A similar age has been obtained for the $\delta^{13}C$ minimum in the *N. dutertrei* record from another EEP site on the Carnegie Ridge (core TR163-31B, 3°37′S, 83°58′W, 3210 m) (*24, 25*), which is overlain by the Peru current. The duration of the $\delta^{13}C$ decrease at TR163-19 is ~4 ky, after which $\delta^{13}C$ gradually increases until the mid- Holocene.

Although a number of age models exist for the Vostok ice core, the age of the pre-event interval in TR163-19, 19.8 cal ky, agrees well with the timing of initial Antarctic warming according to the atmospheric $\delta^{18}O$ age model (*26*). The age of the absolute $\delta^{13}C$ minimum agrees with the timing of this event in South Atlantic upwelled waters off Namibia (13.2 ^{14}C ky) (*4*) and the initial appearance of high $\delta^{13}C$ NADW in the South Atlantic (13.1 ky) (*13*). It

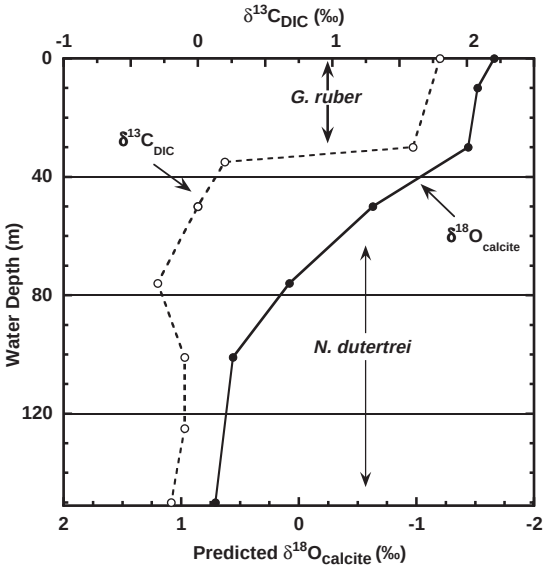


Fig. 1. Water column hydrographic data from the IRONEX cruise, Station 8, November 1993, 92°W, 1°N (*18*) and planktic foraminifera habitat distribution (*19*) near Site TR163-19 in the EEP. *Globigerinoides ruber* resides in the mixed layer whereas *Neogloboquadrina dutertrei* inhabits the deeper thermocline whose chemistry is controlled by the EUC. Predicted $\delta^{18}O_{calcite}$ was calculated from the low light *Orbulina universa* relationship of Bemis *et al.* (*36*) using salinity and temperature data from Station 8 in (*18*). Measurements of $\delta^{13}C_{DIC}$ are from the Panama Basin to the east of TR163-19 (*19*). These gradients reflect the strength of the near-surface pycnocline and chemocline which separate the habitats of *G. ruber* and *N. dutertrei*.

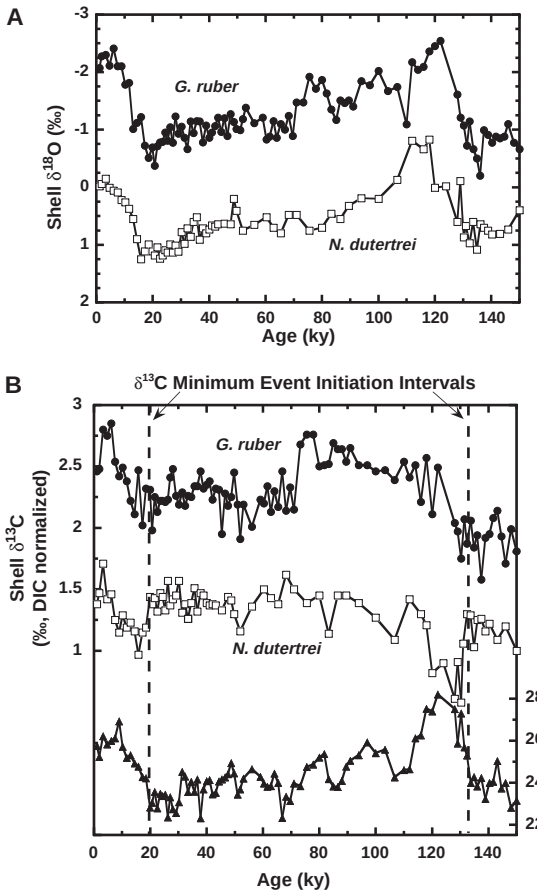


Fig. 2. Measured shell $\delta^{18}O$ (**A**) and DIC-normalized shell $\delta^{13}C$ (**B**) for *G. ruber* (250 to 350 μm fraction) and *N. dutertrei* (>500 μm shell length) at Site TR163-19 during the last 150 ky. *G. ruber* $\delta^{18}O$ and Mg/Ca-derived SST data (B) were published previously (*10*). Note that on both Terminations, the initiation of the $\delta^{13}C$ minimum events occurs at the start of mixed layer warming in the EEP, as indicated by *G. ruber* Mg/Ca. To account for biologically and environmentally controlled offsets (e.g., vital effects) between the two species, the raw $\delta^{13}C$ data here have been normalized to $\delta^{13}C_{DIC}$ using offset corrections of +0.94 and −0.50‰ for *G. ruber* and *N. dutertrei*, respectively (*37*). The chronology for TR163-19 for the last 28 ky has been modified from the original correlation of the *G. ruber* oxygen isotope record to the SPECMAP chronology and a core-top radiocarbon age (*10*) using the two new AMS dates presented in the text. We sampled *G. ruber* at 5-cm resolution (*10*), equivalent to a potential resolution of about 2 ky. We sampled *N. dutertrei* at 10 cm resolution throughout the core with the exception of the last 50 ky and Termination II, which were sampled every 5 cm. The $\delta^{18}O$ and $\delta^{13}C$ differences support a continuous mixed layer and thermocline habitat for these two species. Note that the $\delta^{13}C$ minima on glacial Terminations I and II are absent from the *G. ruber* record, indicating the geochemical environment of the mixed layer is distinct from the EUC dominated thermocline (Fig. 1). Spero *et al.* (*37*) suggest the surface $\delta^{13}C$ signal is not in equilibrium with the atmosphere and may be controlled by a combination of surface productivity changes and advection of surface waters from outside the region.

Downloaded from www.sciencemag.org on November 27, 2006

also corresponds to the age of the high to low $\delta^{13}C$ transition in the deep Caribbean that is thought to reflect the shift in source waters from Glacial North Atlantic Intermediate Water to AAIW (*27, 28*). The agreement among these ^{14}C dates clearly links the $\delta^{13}C$ minimum event to a combination of Southern Ocean warming and changes in thermohaline circulation.

Nitrogen isotopes and other geochemical tracers from Southern Ocean sediments have been used to argue for reduced nutrient supply, increased nitrogen utilization efficiency and increased surface stratification south of the Antarctic polar front during the Last Glacial Maximum (LGM) (*29*). François *et al.* (*29*) reasoned that unlike today, where unstratified waters of the Southern Ocean south of the polar front represent one of the major areas of CO_2 efflux to the atmosphere, the isolation of this CO_2 "leak" zone via stratification could help explain the low pCO_2 levels during the LGM. Modeling results have reinforced this hypothesis, suggesting that LGM pCO_2 levels could result from reduced deepwater ventilation (*30*) associated with a northward shift of the polar easterlies that produced intermediate rather than deep water upwelling (*31*), a combination of winter sea-ice coverage and ice-induced stratification during the summer (*32*), or some other mechanism (*33*). If correct, the $\delta^{13}C_{DIC}$ of late glacial lower CPDW should have decreased (*29*) while that of AAIW and SAMW would have been higher because of decreased nutrient content (*31*). In this regard, very negative glacial deep water $\delta^{13}C$ values are present in benthic foraminifera from the Atlantic sector of the sub-Antarctic Southern Ocean (*13, 34*).

If we can assume that the Southern Ocean was affected by reduced deepwater ventilation at the end of the LGM, then several events should have occurred virtually simultaneously once the Antarctic continent began to warm, sea ice melted back, and deep mixing and convection of lower CPDW was reestablished. First, upwelling and subsequent northward advection of low $\delta^{13}C$ waters to the sub-Antarctic front would have transmitted a low $\delta^{13}C$ signal into the SAMW/AAIW source region. Simultaneously, atmospheric CO_2 concentrations would rise as supersaturated deep waters evolve CO_2 into the atmosphere, and the $\delta^{13}C$ of atmospheric CO_2 would decrease in response to the chemistry of this new outgassing source (*32*). Because these events should have occurred simultaneously, the initiation of the $\delta^{13}C$ decrease would coincide with changes in atmospheric CO_2 (Fig. 3B) and Antarctic temperature (*9*).

We suggest that the $\delta^{13}C$ minima on glacial terminations in EEP records are recording the postglacial expansion of deepwater ventilation and upwelling south of the polar front. The low $\delta^{13}C$ signal derived from Southern Ocean deep water was transmitted into the Indo-Pacific and South Atlantic thermocline, where it was recorded as a decrease in foraminiferal $\delta^{13}C$ (*2*). Because the event required ~4 ky to attain minimum $\delta^{13}C$ values, the establishment of modern mode upwelling may have occurred regionally at first, or could reflect a lag in the mixing time of the low latitude thermocline during a period of thermohaline circulation reorganization. We hypothesize that the $\delta^{13}C$ of the waters feeding SAMW would have started to rise when North Atlantic thermohaline circulation reinitiated and NADW began contributing low nutrient, high $\delta^{13}C$ to the SAMW source region (*13*). Contributing to this $\delta^{13}C$ increase at the sub-Antarctic front would be the general reduction in $^{13}C/^{12}C$ fractionation at the air-sea interface as SST increased (*5*), and the increase in $^{12}CO_2$ uptake as the terrestrial biosphere expanded.

The most compelling support for our hypothesis comes from the agreement in timing among events from different regions. The synchronous initiation of the $\delta^{13}C$ minimum event and SST increase in the Cocos Ridge record and the agreement of the timing of these oceanic events with the start of Antarctic warming and pCO_2 rise as recorded in ice cores links these events to the end-glacial warming of the Southern Ocean. Similarly, the age agreement of the absolute $\delta^{13}C$ minimum at TR163-19 with changes in deep Caribbean and South Atlantic $\delta^{13}C$ (*13, 27*) and the age of the minimum in surface waters of the South Atlantic (*4*) and Peru current (*24, 25*), links these geochemical changes to SAMW/AAIW and the reorganization of thermohaline circulation and NADW production in the North Atlantic.

If our hypothesis is correct, then two additional signals should be present in the geological record. First, in agreement with an earlier suggestion (*32*), the $\delta^{13}C$ of atmospheric CO_2 should decrease as pCO_2 begins to rise on terminations. Both ice core (*9*) and terrestrial carbon data (*8*) show a ~0.5‰ reduction in the $\delta^{13}C$ of CO_2 at the beginning of the last deglaciation (Fig. 3B) that is comparable in magnitude to the $\delta^{13}C$ reduction recorded by *N. dutertrei* at TR163-19. Although the timing of the Taylor Dome pCO_2 event is ~2 ky later than the initiation of the *N. dutertrei* $\delta^{13}C$ minimum event, the offset may reflect a combination of the age uncertainties at TR163-19 due to bioturbation and the models used to estimate the lock-in age of the gas relative to the ice. If, the atmospheric and oceanic $\delta^{13}C$ events are coeval, then it may be possible to use them to link the marine carbon isotope record with ice core gas ages during deglaciations. Based on the existence of a larger marine event during Termination II (Fig. 2B), we would predict that a $\delta^{13}C$ minimum should also be present in Antarctic pCO_2 records at the end of the penultimate glaciation.

Second, records of benthic foraminifera from the Pacific should record the $\delta^{13}C$ minima events at intermediate water depths, but it should be absent from depths that were bathed by CPDW during the glacial. Intermediate and deepwater benthic records from V19-27 (1373 m) and RC13-110 (3231 m) in the EEP (*35*) show that on both Terminations I and II the intermediate water record displays a clear $\delta^{13}C$ minima spike while the deeper record displays a nearly continuous $\delta^{13}C$ rise.

Previous studies have pointed out that benthic-planktic $\Delta\delta^{13}C$ differences contain considerable Milankovich forcing and scale well to the Vostok pCO_2 record (*1*). Perhaps a considerable component of the atmospheric pCO_2–oceanic $\Delta\delta^{13}C$ relationship is due to the strengthening and weakening of deep mixing south of the sub-Antarctic front, as the rate of upwelling, CO_2 leakage to the atmosphere, and thermohaline circulation modified the vertical

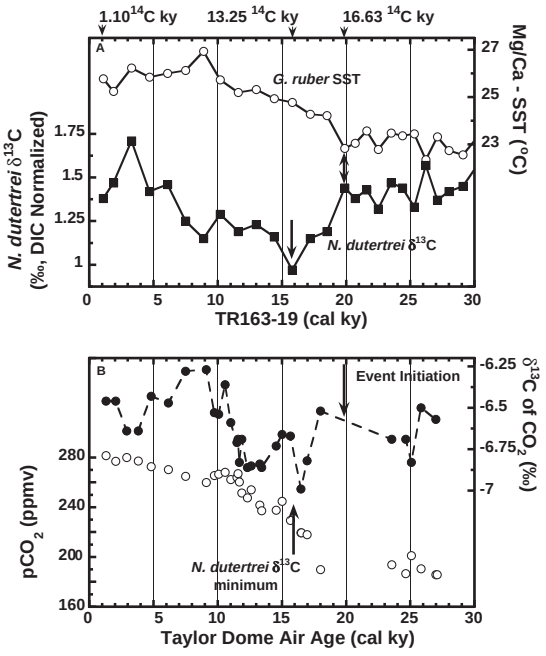


Fig. 3. (**A**) TR163-19 *N. dutertrei* $\delta^{13}C$ and *G. ruber* SST across Termination I. AMS ages (upper arrowheads) correspond to the intervals prior to SST increase and $\delta^{13}C$ decrease and the *N. dutertrei* $\delta^{13}C$ minimum. (**B**) pCO_2 concentration and $\delta^{13}C$ of CO_2 from the Taylor Dome ice core record (*9*). Note that the $\delta^{13}C$ minimum is coincident in the two records, but the onset of the event is older in the sediment record.

Downloaded from www.sciencemag.org on November 27, 2006

$^{13}C/^{12}C$ distribution and changed with Milankovich forcing. In addition, the existence of deglacial $\delta^{13}C$ minima in tropical surface water records (*2, 3*) has been difficult to explain because the nutrient increase implied by the $\delta^{13}C$ shift is not supported by evidence of increased upwelling in these presently nutrient-poor regions (*2*). Because the $\delta^{13}C$ of atmospheric CO_2 was lower at the onset of the deglaciation, tropical surface water $\delta^{13}C_{DIC}$ would have decreased via air-sea equilibration without an accompanying nutrient change. Such a mechanism is analogous to the invasion of low $\delta^{13}C$ anthropogenic CO_2 into the modern surface ocean (*7*). Taken as a whole, the timing and distribution of the deglacial carbon isotope minimum in tropical marine sediments is consistent with a Southern Ocean origin, with advection through intermediate waters and atmospheric equilibration providing the high-latitude–tropical connection.

References and Notes

1. N. J. Shackleton, M. A. Hall, J. Line, C. Shuxi, *Nature* **306**, 319 (1983).
2. D. W. Oppo, R. G. Fairbanks, *Paleoceanography* **4**, 333 (1989).
3. W. B. Curry, T. J. Crowley, *Paleoceanography* **2**, 489 (1987).
4. R. R. Schneider *et al.*, in *Upwelling Systems: Evolution Since the Early Miocene*, C. P. Summerhayes, W. L. Prell, K. C. Emeis, Eds. (Geological Society, London, 1992), pp. 285–297.
5. U. S. Ninnemann, C. D. Charles, *Paleoceanography* **12**, 560 (1997).
6. N. J. Shackleton, in *The Fate of Fossil Fuel CO_2 in the Oceans*, N. R. Andersen, A. Malahoff, Eds. (Plenum, New York, 1977), pp. 401–427.
7. J. Lynch-Stieglitz, R. G. Fairbanks, C. D. Charles, *Paleoceanography* **9**, 7 (1994).
8. B. D. Marino, M. B. McElroy, R. J. Salawitch, W. G. Spaulding, *Nature* **357**, 461 (1992).
9. H. J. Smith, H. Fischer, M. Wahlen, D. Mastroianni, B. Deck, *Nature* **400**, 248 (1999).
10. D. W. Lea, D. K. Pak, H. J. Spero, *Science* **289**, 1719 (2000).
11. M. Tsuchiya, R. Lukas, R. A. Fine, E. Firing, E. J. Lindstrom, *Prog. Oceanogr.* **23**, 101 (1989).
12. R. Lukas, *Prog. Oceanogr.* **16**, 63 (1986).
13. C. D. Charles, R. G. Fairbanks, *Nature* **355**, 416 (1992).
14. J. Toggweiler, D. Dixon, W. S. Broecker, *J. Geophys. Res.* **96**, 20467 (1991).
15. K. Hanawa, L. D. Talley, in *Ocean Circulation and Climate*, G. Siedler, J. Church, Eds. (Academic Press, San Diego, 2001), pp. 373–393.
16. C. D. Charles, R. G. Fairbanks, in *Geological History of the Polar Oceans: Arctic Versus Antarctic*, U. Bleil, J. Thiede, Eds. (Kluwer Academic, Dordrecht, Netherlands, 1990), pp. 519–538.
17. M. Tsuchiya, *Deep-Sea Res. I* **38**, S273 (1991).
18. F. J. Millero, W. Yao, K. Lee, J.-Z. Zhang, D. M. Campbell, *Deep-Sea Res. II* **45**, 1115 (1998).
19. R. G. Fairbanks, M. Sverdlove, R. Free, P. H. Wiebe, A. W. H. Bé, *Nature* **298**, 841 (1982).
20. J. R. Petit *et al.*, *Nature* **399**, 429 (1999).
21. H. Gildor, E. Tziperman, *Paleoceanography* **15**, 605 (2000).
22. K. C. Taylor *et al.*, *Nature* **366**, 549 (1993).
23. Accelerator mass spectrometry (AMS) ^{14}C ages were determined on two samples of monospecific *N. dutertrei* (10 to 12 mg; ~300 shells) at the Center for AMS, Lawrence Livermore National Laboratory. Radiocarbon ages were calibrated to calendar ages using the CALIB program (version 4.3) (http://calib.org/calib/) and a ΔR of 135 ± 40. The two late glacial ages presented here are corrected for an apparent Galapagos surface water reservoir age of 635 years.
24. N. J. Shackleton *et al.*, *Nature* **335**, 708 (1988).
25. Unpublished *N. dutertrei* $\delta^{13}C$ data from TR163-31B were provided by N. J. Shackleton.
26. T. Sowers *et al.*, *Paleoceanography* **8**, 737 (1993).
27. D. W. Oppo, R. G. Fairbanks, *Earth Planet. Sci. Lett.* **86**, 1 (1987).
28. W. S. Broecker *et al.*, *Radiocarbon* **32**, 119 (1990).
29. R. François *et al.*, *Nature* **389**, 929 (1997).
30. J. R. Toggweiler, *Paleoceanography* **14**, 571 (1999).
31. D. M. Sigman, E. A. Boyle, *Nature* **407**, 859 (2000).
32. B. B. Stephens, R. F. Keeling, *Nature* **404**, 171 (2000).
33. M. A. Morales Maqueda, S. Rahmstorf, *Geophys. Res. Lett.* **29**, 10.1029/2001GL013240 (2002).
34. A. Mackensen, M. Rudolph, G. Kuhn, *Global Planet. Change* **30**, 197 (2001).
35. A. C. Mix, N. G. Pisias, W. R. Zahn, C. Lopez, K. Nelson, *Paleoceanography* **6**, 205 (1991).
36. B. E. Bemis, H. J. Spero, J. Bijma, D. W. Lea, *Paleoceanography* **13**, 150 (1998).
37. H. J. Spero *et al.*, in preparation.

38. We thank J. Kennett for samples, J. Bijma, R. Zeebe, A. Wischmeyer, and B. Hoenisch for comments and suggestions, L. Talley for discussion on Pacific ocean circulation, T. Guilderson for AMS dates, E. Kalve and D. Pak for sample preparation, and L. Juranek and D. Winter for technical assistance. F. Millero kindly provided unpublished IRONEX cruise water column data. Supported by NSF grants OCE-9903632 (H.J.S.) and OCE-0117886 (D.W.L.) and a fellowship to H.J.S. from the Hanse Institute for Advanced Study.

27 December 2001; accepted 20 March 2002

Control of the Selectivity of the Aquaporin Water Channel Family by Global Orientational Tuning

Emad Tajkhorshid,[1]* Peter Nollert,[2]*† Morten Ø. Jensen,[1]*‡ Larry J. W. Miercke,[2] Joseph O'Connell,[2] Robert M. Stroud,[2]§ Klaus Schulten[1]§

Aquaporins are transmembrane channels found in cell membranes of all life forms. We examine their apparently paradoxical property, facilitation of efficient permeation of water while excluding protons, which is of critical importance to preserving the electrochemical potential across the cell membrane. We have determined the structure of the *Escherichia coli* aquaglyceroporin GlpF with bound water, in native (2.7 angstroms) and in W48F/F200T mutant (2.1 angstroms) forms, and carried out 12-nanosecond molecular dynamics simulations that define the spatial and temporal probability distribution and orientation of a single file of seven to nine water molecules inside the channel. Two conserved asparagines force a central water molecule to serve strictly as a hydrogen bond donor to its neighboring water molecules. Assisted by the electrostatic potential generated by two half-membrane spanning loops, this dictates opposite orientations of water molecules in the two halves of the channel, and thus prevents the formation of a "proton wire," while permitting rapid water diffusion. Both simulations and observations revealed a more regular distribution of channel water and an increased water permeability for the W48F/F200T mutant.

Efficient permeation of water across cell membranes is mediated by a family of transmembrane water channels called aquaporins (AQPs) (*1, 2*). More than ten different genes encoding AQPs have been identified in the human genome, and their defective forms are known to cause diseases including nephrogenic diabetes insipidus, Sjorgens syndrome, and congenital cataract formation (*3*). They share the remarkable property of effective water conductance at rates close to 10^9 s^{-1} combined with a strict exclusion of all ions including protons (*4*). Aquaglyceroporins such as human AQP7, a glycerol specific channel in adipose tissue, and the *E. coli* glycerol channel, GlpF, belong to a subfamily that possesses the additional capability of passive and stereoselective carbohydrate transport (*5*). The recently determined structure of GlpF at 2.2 Å resolution with three bound glycerol molecules (*6, 7*) explains the channel's specificity and set the stage for molecular dynamics (MD) simulations to reveal the pathway

[1]Theoretical Biophysics Group, Beckman Institute, University of Illinois at Urbana-Champaign, 405 North Mathews, Urbana, IL 61801, USA. [2]Department of Biochemistry and Biophysics, School of Medicine, University of California at San Francisco, San Francisco, CA 94143, USA.

*These authors contributed equally to this work.
†Present address: Emerald BioStructures, Bainbridge Island, WA 98110, USA.
‡Visiting from Membrane and Statistical Physics Group, Department of Chemistry, Technical University of Denmark; present address: Quantum Protein Centre, Department of Physics, Technical University of Denmark, DK-2800 Lyngby, Denmark.
§To whom correspondence should be addressed. E-mail: stroud@msg.ucsf.edu (R.M.S.) or schulte@ks.uiuc.edu (K.S.)

Downloaded from www.sciencemag.org on November 27, 2006